

## Transport in self-assembled molecular wires: Effect of packing and order

Geetha R. Dholakia,<sup>\*,†</sup> Wendy Fan,<sup>†</sup> Jessica Koehne, Jie Han,<sup>†</sup> and M. Meyyappan  
 Center for Nanotechnology, NASA Ames Research Center, Moffett Field, California 94035, USA

(Received 20 November 2003; published 5 April 2004)

We show that orientation, packing, and order play a vital role in determining the current-voltage ( $I$ - $V$ ) characteristics of self-assembled molecular wires, an important issue which can affect the performance of molecular electronic devices. By topographic and tunneling spectroscopic studies on monolayers of a molecule assembled with and without molecular order, we show that competing forces due to the electric field, intermolecular interactions, tip-molecule physisorption, and substrate-molecule chemisorption influence the transport measurements and its reproducibility. We also find that asymmetry in the  $I$ - $V$  is caused both by the molecular structure and the contact geometry.

DOI: 10.1103/PhysRevB.69.153402

PACS number(s): 73.63.-b, 68.37.Ef, 81.16.Dn

Molecular electronics is a nascent field that hopes to overcome the limitations posed by continuing device miniaturization in silicon technology. If single molecules could be chemically tailored to perform specific electronic tasks,<sup>1</sup> their small size, versatility, adaptability, and ability for self-assembly would provide the platform for ultimate nanoelectronic devices. This field has recently become an active area of research spawning a number of experimental and theoretical studies on electronic transport in molecules.<sup>2</sup> However, in applications where a number of molecules have to be addressed as an ensemble, complex molecule-substrate and intermolecular interactions would affect the self-assembly, influencing their collective behavior and hence the transport through them, an issue which has not been sufficiently addressed before.

In this paper we show that packing and order determine the response of a self-assembled monolayer (SAM) to competing interactions and that the presence of molecular order is very important for reproducible transport measurements. Our scanning tunneling microscopy and spectroscopy (STM/S) results on two types of monolayers formed from the same molecular wire, with and without molecular order, reveal the effect of these competing interactions on the  $I$ - $V$ s and also show that asymmetric molecular structures and large junction resistances result in asymmetric  $I$ - $V$ s. Our  $I$ - $V$ s also highlight the importance of performing transport measurements on SAMs within optimal limits of field and current. The molecule under study, an oligo(phenylene ethynylene) or OPE [Fig. 1(a) inset], was chosen for its conjugated rigid rod structure.<sup>3</sup> Since its derivatives have shown NDR (Ref. 4)  $I$ - $V$  of this molecule should give an estimate of transport through the molecular backbone. Previous studies on this molecule have focused on self-assembly,<sup>5</sup> stochastic switching when inserted in an alkanethiol matrix<sup>6</sup> and the effect of contacts on transport,<sup>7</sup> but none have focused on the relationship between the presence of order in the monolayer and transport. Our results are relevant for transport measurements on any SAM.

Two different approaches were used for self-assembling the molecule on Au(111),<sup>8</sup> yielding a disordered (SAM A) (Ref. 9) and an ordered (SAM B) monolayer.<sup>5,10</sup> After immersion for about 24 h in an inert argon atmosphere, the films were rinsed in the pure solvent to remove any phys-

isorbed multilayers, blown dry in a stream of argon and immediately transferred to the STM chamber<sup>11</sup> and pumped to vacuum. All the measurements were performed in a vacuum of  $\approx 10^{-6}$  mbar. Ellipsometry and x-ray photoemission spectroscopy (XPS) were used to confirm the thickness and chemical identity of the SAM. Mechanically cut Pt/Ir tips were used for imaging, with the bias applied to the sample. The topographic images were obtained in the constant current mode with large tunnel junction impedances of 100 G $\Omega$  to avoid destructive tip-surface interactions.

Figure 1 shows representative topographic images obtained from SAM A and B, illustrating the difference in their packing and order. Figure 1(a) is a  $1 \times 1 \mu\text{m}^2$  scan of SAM A. The image shows "etch pits" typical of thiol chemisorption on Au substrates.<sup>12</sup> Smaller range scans show featureless images and exhibit no long-range molecular ordering in spite of using a variety of imaging conditions. Figure 1(b) is a  $50 \times 50 \text{ nm}^2$  image showing the underlying Au(111) terrace but no order. Figure 1(c) is a  $4.4 \times 5.2 \text{ nm}^2$  scan also show-

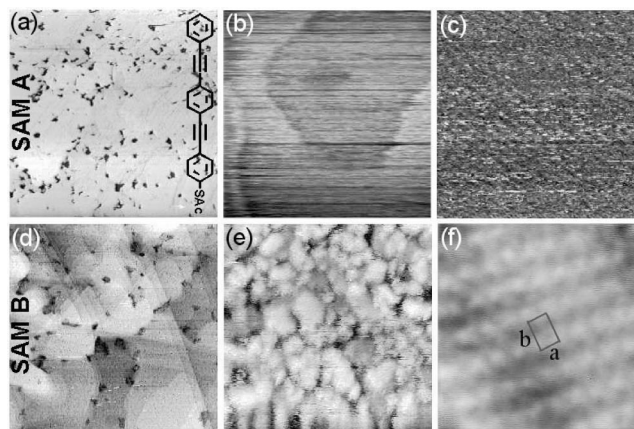


FIG. 1. Topography of disordered (SAM A) and ordered (SAM B) monolayers. (a)  $1 \times 1 \mu\text{m}^2$  image of SAM A showing etch pits. Inset gives the schematic of the molecule. SAc refers to the thioacetate group. (b) and (c) are  $50 \times 50 \text{ nm}^2$  and  $4.4 \times 5.2 \text{ nm}^2$  images of SAM A illustrating the lack of order. (d)  $1 \times 1 \mu\text{m}^2$  image of SAM B showing etch pits and domains. (e)  $50 \times 50 \text{ nm}^2$  image of SAM B within the domains showing small grains having ordered molecular rows. (f)  $5.2 \times 5.2 \text{ nm}^2$  molecular resolution image within a grain. Rectangle marks the  $0.55 \times 0.79 \text{ nm}^2$  unit cell.

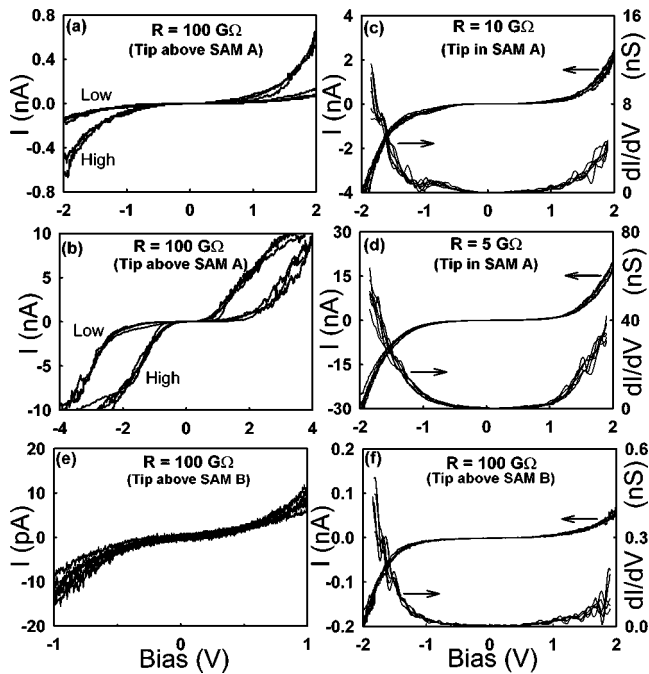


FIG. 2. STS on SAM A and B. (a), (b):  $I$ - $V$ s of disordered SAM A in two scan ranges (tip above monolayer). They show large deviations from the set point (10 pA/1 V) possibly due to changes in orientation of the molecule with the tip. (c), (d): six reproducible  $I$ - $V$ s each, obtained at different locations of SAM A for two junction resistances (tip in the monolayer). Strong tip-molecule physisorption here precludes the orientation change. The  $dI/dV$ s show a conductance gap and in (c) a strong feature at  $\approx -1$  V. (e), (f):  $I$ - $V$ s on ordered SAM B in two scan ranges (tip above monolayer). Each curve is from different locations within the ordered grains. Ordered packing of SAM B results in stronger intermolecular interactions which resist orientation change under a field, resulting in the curves conforming to the set point. The  $I$ - $V$ s (and  $dI/dV$ s) are asymmetric. This arises from the inherent structural asymmetry in the molecule and unequal contacts. The asymmetry decreases with decreasing  $R$ .

ing no molecular periodicity. This suggests that SAM A does not self-assemble into an ordered monolayer. Figures 1(d), 1(e), and 1(f) are topographic images of SAM B in various scan ranges comparable with those shown for SAM A. Figure 1(d) is a  $1 \times 1 \mu\text{m}^2$  scan of SAM B also showing etch pits and the underlying Au terraces, but also large domains. The important difference from SAM A is that scans within these large domains show dense clusters of small grains, typically 3–8 nm in diameter. Figure 1(e) illustrates this in a  $50 \times 50 \text{ nm}^2$  region. Ordered rows of atoms can be discerned within each of the small grains. Figure 1(f) ( $5.2 \times 5.2 \text{ nm}^2$ ) clearly shows molecular ordering within one such grain. The marked rectangular unit cell gives lattice constants  $a = 0.55 \text{ nm}$ ,  $b = 0.79 \text{ nm}$ , which agrees well with a previous UHV STM study.<sup>5</sup>

In the rest of this paper we demonstrate that the presence or absence of long-range order in the monolayer affects the tunneling spectroscopic measurements. STS measurements (Fig. 2) are performed by switching off scanning and feedback and recording the tunnel current  $I$  as a function of the applied bias voltage  $V$ , with seven  $I$ - $V$ s averaged at a specific

location of the SAM to yield the single  $I$ - $V$  curve plotted in the figures. Each of these  $I$ - $V$ s shown in the figures has been obtained at different locations of the SAM for statistical completeness. The  $I$ - $V$ s of disordered SAM A are shown in Figs. 2(a)–2(d), while Figs. 2(e)–2(f) are of the ordered SAM B.

Figure 2(a) illustrates typical  $I$ - $V$ s in a  $\pm 2$  V scan range, obtained at different locations with a high tunnel junction resistance  $R$  of  $100 \text{ G}\Omega$  (dc bias = 1 V;  $I = 10 \text{ pA}$ ), with the tip positioned well above the monolayer. From these curves it is immediately apparent that the  $I$ - $V$ s are not very reproducible and that the tunnel current does not always conform to the set point. In fact analysis of numerous sets of  $I$ - $V$ s (obtained using many tips and from different samples to rule out artifacts due to a specific tip or a sample) show that a range of currents from “low” to “high” are obtained for a given set point bias, instead of all the  $I$ - $V$ s conforming to the set point current. Low curves typically conform to the set point, while the high curves deviate by as much as an order of magnitude. Figure 2(b) illustrates the effect of increasing scan range ( $\pm 4$  V) on the  $I$ - $V$ s, showing  $I$  values as large as 1 nA for the high curves for the same  $R$ .

Since each  $I$ - $V$  is an average of many curves obtained while the feedback is turned off (typically  $< 1.5$  s), a variation in the tip-SAM tunneling distance “ $d$ ” or an intrinsic change in the molecule during data acquisition will reflect as a change in the tunnel current from the set point value. In the following sections we determine the factors that affect the SAM  $I$ - $V$  reproducibility. We find that the extent of the current deviation from the set point depends on the degree of order in the monolayer and for a given monolayer it depends on various parameters such as the scan range and the junction resistance.

Thickness measurements on the SAM A obtained from both ellipsometry and XPS give values  $\approx 1.4 \text{ nm}$ , which is smaller than the molecule’s length ( $\approx 2 \text{ nm}$ ), indicating that it is tilted from the surface normal. Further, the fact that molecular resolution could never be obtained on these films shows that the surface is disordered. Local fields in a STM configuration can be as large as  $10^7 \text{ V/cm}$ . Such high fields can disrupt intermolecular forces in disordered SAM’s and interact with molecular dipoles, causing them to tilt and align themselves along the field. Such a movement *during* the course of an  $I$ - $V$  measurement would alter the tunneling distance  $d$ , varying the effective  $R$ . Exponential dependence of  $I$  on  $d$  would result in large  $I$  variations. Modeling results on smaller thiols show that apart from a mere change in the effective  $R$ , tilting of the molecule will also affect the Au-S orbital hybridization, due to the orientational dependence of the  $S p$  orbitals, resulting in qualitatively similar variations in  $I$ - $V$ .<sup>13</sup> Similar results are also expected for the OPE’s. The fact that the deviations in  $I$  from the set point increase on increasing the scan range [Fig. 2(b)] proves that strong fields disrupt intermolecular interactions and perturb the molecular packing, thus affecting the  $I$ - $V$  measurements on disordered SAMs.

From STS measurements as a function of the tip height above the SAM, spanning a range of junction resistances in

which the tip is positioned well above the molecules to when it is within the SAM, we try to ascertain if the current variations are due to changes intrinsic to the molecule and its interaction with the substrate. Figures 2(c) and 2(d) show two sets of six  $I$ - $V$ s, each acquired at different locations on SAM A, at smaller  $R$ 's of 10 G $\Omega$  (Bias=1 V;  $I$ =0.1 nA) and 5 G $\Omega$  (Bias=0.5 V;  $I$ =0.1 nA), respectively. For these  $R$ 's the tip is buried in the monolayer, evident from a change in the slope of the  $I$ - $d$  curve when the tip touches the SAM and also from noisy images due to destructive tip-SAM interactions. Interestingly, all these  $I$ - $V$ s confirm to the set point. This indicates that there is perhaps no intrinsic, dynamic change in the molecule during the STS scans, since any such change would reflect in the  $I$ - $V$ s. For these 2 nm long molecules, the effect of burying the tip in the SAM probably causes them to attach to the tip by physisorption, constraining tilting and movement, explaining the reproducibility. It is to be noted that while the top of the molecule is locked by physisorption to the tip, the sulphur end is free to move laterally on the Au(111) surface, if it were energetically favorable. The reproducible  $I$ - $V$ s of SAM B and SAM A (5 and 10 G $\Omega$ ) indicate that for small scan ranges such lateral movement does not occur. However, increasing the scan range to  $\pm 4$  V causes the  $I$  to vary, indicating that at sufficiently high fields either the tip-molecule physisorption and/or the Au-S bond is perturbed.

Figures 2(e) and 2(f) are STS results of ordered SAM B, obtained at a  $R$  of 100 G $\Omega$  (dc bias=1 V;  $I$ =10 pA). Eight and five curves, respectively in the  $\pm 1$  V and  $\pm 2$  V scan ranges are shown. Each was obtained at different locations inside the small grains showing ordered rows of atoms. Clearly, the most important difference from SAM A is that the curves here conform to the set point, showing stable and reproducible current-voltage characteristics. Since the experimental conditions, such as the scan range and  $R$  [Fig. 2(f)] are the same as for SAM A [Fig. 2(a)], the reproducibility in this case would imply that the tip-molecule distance is not altered during the measurement. The reason for this is clear from the STM images of SAM B, Figs. 1(e) and 1(f). Close packing of the molecules here in a highly ordered structure results in intermolecular forces strong enough to constrain them from moving under an applied field, provided the current and field values are not so large as to disrupt these interactions. While in the case of SAM A, the disorder in the monolayer and the subsequent absence of close packing permits molecular motion and tilting in the presence of a perturbing field.

Although the absolute magnitude of the tunneling current is small, the field and current density through the molecules in such a transport measurement can be quite large and this can affect the subtle balance between intermolecular and molecule-substrate interactions and even lead to conformational changes, all of which will affect the reliability and reproducibility of the measurements. Thus, it is important to determine the optimal parameters for performing nondestructive measurements. Concurrent imaging after the STS scans on SAM B showed no evidence of tip or field induced damage to the ordered monolayers up to  $\pm 2$  V. However increasing the scan range to  $\pm 3$  V results in blurring of atomic

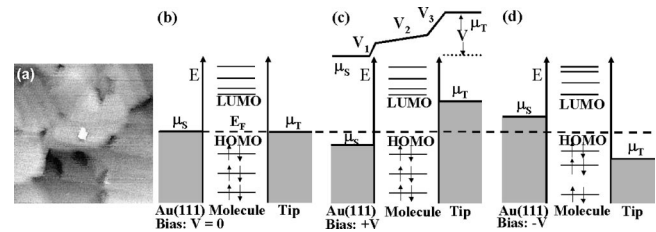


FIG. 3. (a)  $500 \times 500$  nm $^2$  image showing a 35 nm bright region of damage subsequent to  $\pm 4$  V  $I$ - $V$  scans. (b)–(d) schematically show the energy levels and the potential drops across the SAM junction. (b) At equilibrium a common  $E_F$ , typically lying in the HOMO-LUMO gap, is established for the entire system. (c) Under bias  $V$ , the contact electrochemical potentials  $\mu_S$  (Au) and  $\mu_T$  (tip) split by  $eV$ . The relative potential drops across the junction are shown. The strong chemisorption of the molecule to Au compared to its weak coupling to the tip results in  $V_1 < V_3$ . For small biases,  $\mu$  lies in the gap and there is just a small current due to off resonant tunneling, showing up as a gap in the  $dI/dV$ . When the applied bias is sufficiently large for one of the  $\mu$  to cross a molecular level, there is an onset of current. (d) Bias reversal: Inherent molecular asymmetry and different coupling strengths to the leads results in different onsets for the current under bias reversal and hence to  $I$ - $V$  asymmetry.

resolution and in current deviations from the set point. Further increasing the scan range to  $\pm 4$  V causes drastic tunnel current instabilities. STM imaging over the relevant region, shown as a  $500 \times 500$  nm $^2$  image in Fig. 3(a), reveals a large bright region of damage  $\approx 35$  nm, caused by bunching of the molecules due to the dissociation of the S-Au bond at high fields and currents. Such dissociation of molecules from the surface is also caused by voltage pulses in STM SAM lithography. Hence stable and reproducible STM/S measurements on the SAMs require large junction resistances (low electric fields) and small voltage scans (typically within  $\pm 2$  V).

Having explored the effect of packing and order of the SAMs on the  $I$ - $V$ s, we look at a few other interesting aspects of our transport measurements such as symmetry of the  $I$ - $V$ s w.r.t bias inversion. Symmetric  $I$ - $V$ s are obtained for small scan ranges, where the current is mostly due to off resonant tunneling [Fig. 2(e)]. For larger scan ranges [Fig. 2(f)], it becomes markedly asymmetric, with larger  $I$  at negative biases. The asymmetry varies also with junction resistance, decreasing with decreasing  $R$ . The origin of asymmetry can be understood from the schematic energy diagram shown in Fig. 3. Large  $R$  in STM measurements implies asymmetric coupling to the leads (tip-molecule: weakly coupled; Au(111)-molecule: strongly coupled) resulting in different contact resistances and potential drops across the two interfaces and hence in asymmetric  $I$ - $V$ s. However, the largest contribution to asymmetry is due to the inherent asymmetry in the molecular structure, which has a sulphur at just one end. Thus, the wave functions and the energy levels of the molecule coupling to the contacts and their Stark shifts are different on bias reversal. This leads to asymmetric  $I$ - $V$ s, illustrated schematically in Figs. 3(c) and 3(d). Thus, even on contact with the monolayer, the  $I$ - $V$ s are asymmetric [Figs. 2(c) and 2(d)]. These issues have been theoretically considered extensively.<sup>14,15</sup> Asymmetry produced by contact ma-

nipulation has also been observed in break junction experiments.<sup>16</sup> Modeling has shown that unequal contacts can also lead to differential charging and a consequent shifting of the energy levels which will further contribute to asymmetry.<sup>17</sup> In fact, the  $I$ - $V$ s in Fig. 2(f) qualitatively look very similar to these modeling results.

The differential conductance  $dI/dV$ , calculated numerically from the  $I$ - $V$ s are shown in Fig. 2 referenced to the right axis. They show a gap in the conductance around zero bias arising from off resonant tunneling.<sup>18</sup> The smooth variation of the  $dI/dV$ s implies that for these  $\pm 2$  V scans, the contacts  $\mu$  have not yet aligned with a molecular energy level for resonant tunneling to occur. Interestingly, all the  $dI/dV$ s obtained at different locations of disordered SAM A at 10 G $\Omega$ , where the tip is in the monolayer, show a consistent feature at  $\approx -1$  V. This is probably due to the spatial distribution a molecular orbital at this  $R$  coupling strongly to the tip.

In conclusion, by concurrent STM/STS measurements we have demonstrated the importance of molecular packing, order, and orientation in self-assembled molecular wires on its response to competing forces due to the applied electric field, intermolecular forces, tip/molecule/substrate interactions and shown that this has consequences on the transport measurements and its reproducibility. The STS results also illustrate the importance of molecular structure and contact resistance on the rectifying behavior of the  $I$ - $V$ s. This study highlights the importance of fluctuations and dynamics in the SAM's which have to be considered in the design and performance of any molecular electronic device having an ensemble of molecules, since self-assembly happens to be essentially a statistically driven process.

We thank J. R. Williams for XPS and ellipsometry measurements. G. R. D thanks M. P. Anantram, A. W. Ghosh, N. Mingo, and M. Samanta for stimulating discussions. Work by ELORET authors was supported by a NASA contract.

\*Corresponding author. Email address:

gdholakia@mail.arc.nasa.gov

<sup>†</sup>Also at ELORET, Sunnyvale, CA 94087.

<sup>1</sup>A. Aviram and M.A. Ratner, Chem. Phys. Lett. **29**, 277 (1974).

<sup>2</sup>M.A. Ratner, Mater. Today **5**, 20 (2002); J.R. Heath and M.A. Ratner, Phys. Today **56** (5), 43 (2003).

<sup>3</sup>For the synthesis procedure, see K. Sonogashira, Y. Tohda, and N. Hagihara, Tetrahedron Lett. **50**, 4467 (1975); R. Wu, J.S. Schumm, D.L. Pearson, and J.M. Tour, J. Org. Chem. **61**, 6906 (1996).

<sup>4</sup>J. Chen, M.A. Reed, A.M. Rawlett, and J.M. Tour, Science **286**, 1550 (1999).

<sup>5</sup>G. Yang, Y. Qian, C. Engtrakul, L.R. Sita, and G. Liu, J. Phys. Chem. B **104**, 9059 (2000).

<sup>6</sup>Z.J. Donhauser, B.A. Mantooth, K.F. Kelly, L.A. Bumm, J.D. Monnell, J.J. Stapleton, D.W. Price, A.M. Rawlett, D.L. Allara, J.M. Tour, and P.S. Weiss, Science **292**, 2303 (2001).

<sup>7</sup>J.G. Kushmerick, D.B. Holt, J.C. Yang, J. Naciri, M.H. Moore, and R. Shashidhar, Phys. Rev. Lett. **89**, 086802 (2002).

<sup>8</sup>Au(111) substrate is prepared just prior to immersion in the organic solution by hydrogen flame annealing a Au\mica film (Molecular Imaging Corp., Arizona).

<sup>9</sup>SAM A formed from 1 mM solution of the molecule in tetrahydrofuran, with *in situ* deprotection of the thioacetate group by  $\text{NH}_4\text{OH}$ , similar to the procedure given in J.M. Tour *et al.*, J. Am. Chem. Soc. **117**, 9529 (1995).

<sup>10</sup>SAM B was formed directly from the thiol analog of the molecule in a 0.1 mM solution in dichloromethane. R.P. Hsung, J.R. Babcock, C.E.D. Chidsey, and L.R. Sita, Tetrahedron Lett. **36**, 4525 (1995).

<sup>11</sup>Oxford Instruments mini cryo STM, UK.

<sup>12</sup>C. Schonenberger, J.A.M. Sondag-Huethorst, J. Jorritsma, and L.G.J. Fokink, Langmuir **10**, 611 (1994).

<sup>13</sup>A.M. Bratkovsky and P.E. Kornilovitch, Phys. Rev. B **67**, 115307 (2003).

<sup>14</sup>S. Datta, W. Tian, S. Hong, R. Reifenberger, J.I. Henderson, and C.P. Kubiak, Phys. Rev. Lett. **79**, 2530 (1997); W. Tian, S. Datta, S. Hong, R. Reifenberger, J.I. Henderson, and C.P. Kubiak, J. Chem. Phys. **109**, 2874 (1998).

<sup>15</sup>Y. Xue and M.A. Ratner, Phys. Rev. B **68**, 115406 (2003).

<sup>16</sup>J. Reichert, R. Ochs, D. Beckmann, H.B. Weber, M. Mayor, and H.v. Löhneysen, Phys. Rev. Lett. **88**, 176804 (2002).

<sup>17</sup>A.W. Ghosh, F. Zahid, P.S. Damle, and S. Datta, cond-mat/0202519 (unpublished).

<sup>18</sup>The gap reflects the energy difference between the equilibrium  $E_F$  of the contacts and the molecular level closest to it. Single electron tunneling effects such as Coulomb blockade are unlikely to be present here due to the strong chemisorption of the molecule to Au(111), which results in charging energies (0.7 eV for a sphere of 2 nm)  $\approx$  energy level broadening due to contacts (0.2 eV, Ref. 15).